JOURNAL OF GUIDANCE, CONTROL, AND DYNAMICS
Vol. 33, No. 6, November–December 2010

Engineering Notes

Extension of the Sun-Synchronous Orbit

Malcolm Macdonald* and Robert McKay†
University of Strathclyde,
Glasgow, Scotland G1 1XJ, United Kingdom
Massimiliano Vasile‡
University of Glasgow,
Glasgow, Scotland G12 8QQ, United Kingdom
and
François Bosquillon de Frescheville§
ESA, 64293 Darmstadt, Germany

DOI: 10.2514/1.49011

Nomenclature

a	=	semimajor axis
$C_{n,m}$	=	harmonic coefficient of body
e	=	eccentricity
$\mathbf{F}$	=	low-thrust perturbation
F_N	=	low-thrust out-of-orbit plane perturbation scalar
F_R	=	low-thrust radial perturbation scalar
G	=	universal gravitational constant
J_n	=	constant from within the Legendre polynomials
M_E	=	mass of Earth
N	=	normal perturbation acceleration
n	=	number of revolutions/orbits per day
$P_{n,m}$	=	Legendre polynomials
p	=	semilatus rectum
R	=	radial perturbation acceleration
r, $\mathbf{r}$	=	orbit radius,
$R_\oplus$	=	mean volumetric radius of Earth
$\dot{}$	=	velocity
$\ddot{}$	=	acceleration

I. Introduction

THROUGH careful consideration of the orbit perturbation force due to the oblate nature of the primary body a secular variation of the ascending node angle of a near-polar orbit can be induced without expulsion of propellant. Resultantly, the orbit perturbations can be used to maintain the orbit plane in, for example, a near-perpendicular (or at any other angle) alignment to the sun line throughout the full year of the primary body; such orbits are normally termed sun-synchronous orbits [1,2]. Sun-synchronous orbits about the Earth are typically near-circular low Earth orbits (LEOs), with an altitude of less than 1500 km. It is normal to design an LEO such that the orbit period is synchronized with the rotation of the Earth's surface over a given period, such that a repeating ground track is established. A repeating ground track, together with the near-constant illumination conditions of the ground track when observed from a sun-synchronous orbit, enables repeat observations of a target over an extended period under similar illumination conditions [1,2]. For this reason, sun-synchronous orbits are extensively used by Earth observation (EO) platforms, currently including the Environmental Satellite (ENVISAT), the second European Remote Sensing satellite (ERS-2), and many more.

By definition, a given sun-synchronous orbit is a finite resource similar to a geostationary orbit. A typical characterizing parameter of a sun-synchronous orbit is the mean local solar time (MLST) at descending node, with a typical value of 1030 h. Note that ERS-1 and ERS-2 use an MLST at descending node of 1030 h ± 5 min, while ENVISAT uses a 1000 h ± 5 min MLST at descending node [3]. Following selection of the MLST at descending node and for a given desired repeat ground track, the orbit period and hence the semimajor axis are fixed; thereafter, assuming a circular orbit is desired, it is found that only a single orbit inclination will enable a sun-synchronous orbit [2]. As such, only a few spacecraft can populate a given repeat-ground-track sun-synchronous orbit without compromise: for example, on the MLST at descending node. Indeed, a notable feature of ongoing studies by the ENVISAT Post Launch Support Office is the desire to ensure sufficient propellant remains at end of mission for reorbiting to a graveyard orbit to ensure that the orbital slot is available for future missions [4].

An extension to the sun-synchronous orbit is considered using an undefined, non-orientation-constrained, low-thrust propulsion system. Initially, the low-thrust propulsion system will be considered for the free selection of orbit inclination and altitude while maintaining the sun-synchronous condition. Subsequently, the maintenance of a given sun-synchronous repeat ground track will be considered, using the low-thrust propulsion system to enable the free selection of orbit altitude. An analytical expression will be developed to describe these extensions before then validating the analytical expressions within a numerical simulation of a spacecraft orbit. Finally, an analysis will be presented on transfer and injection trajectories to these orbits.

II. Satellite Motion About an Oblate Body

The gravitational potential may be written as [1]

$$U(r,\beta,\lambda) = \frac{\mu}{r}\sum_{n=0}^{\infty}\sum_{m=0}^{\infty}\left(\frac{R_E}{r}\right)^n (C_{n,m}\cos m\lambda + S_{n,m}\sin m\lambda)P_{n,m}\sin\beta \tag{1}$$

which, for a body possessing axial symmetry, may be written for a point external to it, as

$$U(r,\beta) = \frac{\mu}{r}\left[1 - \sum_{n=0}^{\infty} J_n\left(\frac{R_E}{r}\right)^n P_n \sin\beta\right] \tag{2}$$

This assumption is valid for Earth, as the influence of periodic effects (tesseral and sectorial harmonics) can be neglected for most orbits, with the notable exception of geostationary orbits. It is thereafter found that

Received 21 January 2010; revision received 25 July 2010; accepted for publication 25 July 2010.

*Associate Director, Advanced Space Concepts Laboratory, Department of Mechanical Engineering; malcolm.macdonald.102@strath.ac.uk. Senior Member AIAA.

†Research Fellow, Advanced Space Concepts Laboratory, Department of Mechanical Engineering; Robert.j.mckay@strath.ac.uk.

‡Senior Lecturer, Space Advanced Research Team, Department of Aerospace Engineering; m.vasile@aero.gla.ac.uk.

§Future Studies Operations Concept Engineer, European Space Operations Centre, Human Spaceflight and Exploration Department, Robert-Bosch-Strasse 5; Francois.Bosquillon.de.Frescheville@esa.int.

$$U(r,\beta)=\frac{\mu}{r}\left[1-J_2\frac{1}{2}\left(\frac{R_\oplus}{r}\right)^2(3\sin^2\beta-1)-J_3\frac{1}{2}\left(\frac{R_\oplus}{r}\right)^3(5\sin^3\beta-3\sin\beta)-J_4\frac{1}{8}\left(\frac{R_\oplus}{r}\right)^4(3-30\sin^2\beta+35\sin^2\beta)-\cdots\right] \quad (3)$$

Using spherical triangle laws and considering only the first-order terms, Eq. (3) reduces to

$$U(r,\beta)=U_o+U_p=\frac{\mu}{r}-J_2\frac{\mu R_\oplus^2}{2r^3}(3\sin^2 i\sin^2 u-1) \quad (4)$$

A sun-synchronous orbit requires that the rate of change of the ascending node match the mean rate of rotation of the sun within an Earth-centered inertial reference frame ($2\pi/365.25$). The ascending node angle can be described within an Earth-centered inertial reference frame through the Gaussian form of the variational equations of the classic orbital elements. Selecting the positioning-fixing element to be the true anomaly, the rate of change of the ascending node angle is [5]

$$\frac{\mathrm{d}\Omega}{\mathrm{d}v}=\frac{r^3}{\mu p\sin i}\sin(v+\bar{\omega})N \quad (5)$$

Thus, U_p within Eq. (4) is required in terms of the spacecraft-centered RTN coordinate system and is obtained by differentiation of the potential with respect to the spacecraft-centered RTN coordinate system. The disturbing force components due to J_2 are thus

$$R_{J_2}=\frac{3}{2}J_2\frac{\mu R_\oplus^2}{r^4}(3\sin^2 i\sin^2 u-1) \quad (6)$$

$$T_{J_2}=-\frac{3}{2}J_2\frac{\mu R_\oplus^2}{r^4}\sin^2 i\sin^2 u \quad (7)$$

$$N_{J_2}=-\frac{3}{2}J_2\frac{\mu R_\oplus^2}{r^4}\sin 2i\sin u \quad (8)$$

Through a combination of Eqs. (5) and (8), and assuming that the change in other orbit elements is small over the integral, the standard sun-synchronous orbit can be found as

$$i=\cos^{-1}\left[-\frac{2}{3}\frac{\Delta\Omega}{J_2}\frac{a^{7/2}(1-e^2)^2}{R_\oplus^2\sqrt{\mu}}\right] \quad (9)$$

where $\Delta\Omega$ is the mean rotation rate of the sun within an Earth-centered inertial reference frame per second.

III. Low-Thrust Rotation of Ascending Node Angle with J_2

From Eq. (5), and noting that $\sin i\geq 0$ for $0\leq i<\pi$, a secular variation of the ascending node angle over the orbit period is obtained when the low-thrust propulsion system provides an out-of-plane perturbation that switches sign as a function of $\sin(v+\bar{\omega})$ [6]. The combined J_2 and low-thrust out-of-plane perturbation is thus

$$N=-\frac{3}{2}J_2\frac{\mu R_\oplus^2}{r^4}\sin 2i\sin u+F_N\mathrm{sgn}[\sin(v+\bar{\omega})] \quad (10)$$

Thereafter, noting that

$$r=\frac{p}{1+e\cos v} \quad (11)$$

the variation of ascending node angle over the orbit period can be found to be

$$(\Delta\Omega)_0^{2\pi}=\frac{p^2}{\mu\sin i}F_N\int_0^{2\pi}\frac{\sin(v+\bar{\omega})}{(1+e\cos v)^3}\mathrm{sgn}[\sin(v+\bar{\omega})],\,\mathrm{d}v-3J_2\left(\frac{R_\oplus}{p}\right)^2\cos i\int_0^{2\pi}\sin^2(v+\bar{\omega})(1+e\cos v),\,\mathrm{d}v \quad (12)$$

with the second integral on the right-hand side of Eq. (12) equaling π. To solve the first integral, independent of the physical meaning of the variables, it is assumed that $0\leq e<1$. Thereafter, Eq. (12) becomes

$$(\Delta\Omega)_0^{2\pi}=\frac{4p^2}{\mu(-1+e^2)^2}\frac{\cos\bar{\omega}}{\sin i}F_N-3\pi J_2\left(\frac{R_\oplus}{p}\right)^2\cos i \quad (13)$$

Switching the rate of change of ascending node angle per rotation to per second and rearranging, Eq. (13) then becomes

$$\Delta\Omega=\frac{1}{2\pi}\left[4\frac{\cos\bar{\omega}}{\sin i}\sqrt{\frac{a}{\mu}}F_N-\frac{3\pi J_2\sqrt{\mu}\cos i}{\sqrt{a^3}}\left(\frac{R_\oplus}{p}\right)^2\right] \quad (14)$$

Equation (14) can be solved analytically for the semimajor axis. However, as the function has eight roots, such a derivation would be

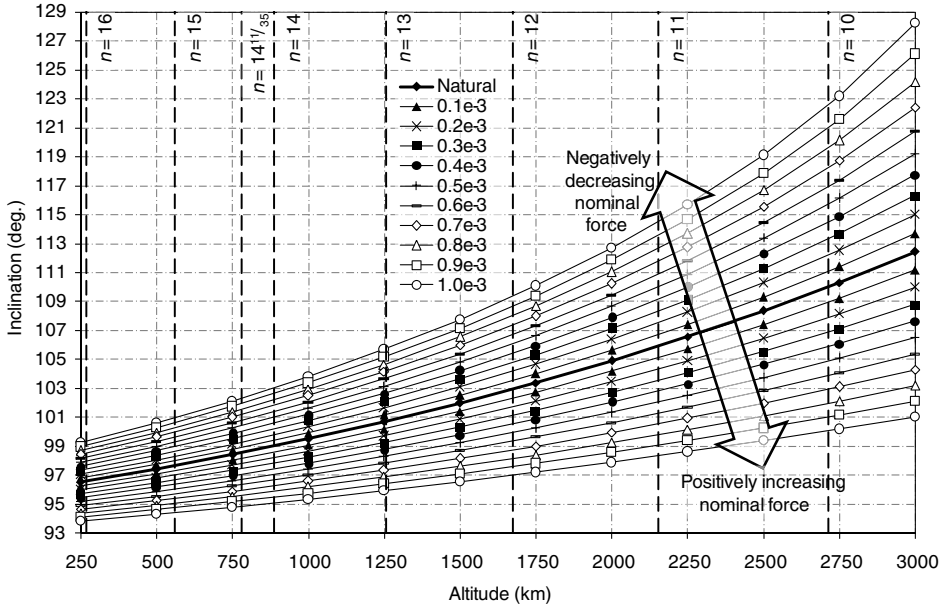

Fig. 1 Sun-synchronous circular orbits with continuous acceleration over a range of values from −1 to 1 mm s^{-2}, contours of number of revolutions per day (n) are also shown.

convoluted, and it is solved numerically herein, allowing determination of the enabled sun-synchronous orbits over a range of semilatus rectum and inclination for a given continuous-low-thrust perturbation following the switching control law detailed above.

Assuming a circular orbit, Eq. (14) is solved numerically within Fig. 1. From Fig. 1, it is seen that for a given altitude the addition of a continuous-low-thrust perturbation enables the use of different orbit inclinations. For example, at $n = 15$ the natural sun-synchronous orbit has an altitude of approximately 561 km, assuming mean volumetric radius of Earth, and inclination of 97.6 deg. However, by application of a continuous-low-thrust perturbation of a magnitude of 0.34 mm s^{-2}, the sun-synchronous orbit can be shifted to $n = 14$ and altitude of 888 km while maintaining the same orbit inclination.

IV. Displaced Sun-Synchronous Orbits

The use of continuous low thrust has been shown to enable extension of sun-synchronous orbits to alternative inclinations for a given repeat cycle. However, a continuous-low-thrust propulsion system can be used to further displace the orbit from those derived using Eq. (14), enabling the orbit altitude to be varied for a given repeat ground track through consideration of displaced two-body orbits. A displaced two-body orbit is an orbit that does not satisfy the conditions of a Keplerian orbit, instead using a low-thrust propulsion system to counteract the effects of gravity and to, for example, orbit at a period consistent with a different orbit semimajor axis. Thus, sun-synchronous orbits (natural or extended) can be displaced such that the orbit altitude is changed without impacting the orbit period, hence maintaining a desired repeat cycle, but at an inclination and altitude of choice. A displaced orbit in the two-body problem with an orbit period fixed by the reference orbit is termed a type-III displaced orbit [7,8].

The equation of motion of a satellite in the rotating reference frame, as shown in Fig. 2, may be written as

$$\ddot{\mathbf{r}} + 2\boldsymbol{\omega} \times \dot{\mathbf{r}} = -\nabla U + \mathbf{F} \tag{15}$$

It is noted that within Fig. 2 the out-of-plane displacement is assumed to be from an equatorial orbit: i.e., inclination of zero. However, as the inclination does not alter the analysis, it can be considered a free parameter, thus allowing inclination to be considered separately, as per a sun-synchronous orbit. From [7,8], and assuming a circular orbit, Eq. (15) reduces to

$$\nabla U = \mathbf{F} \tag{16}$$

where

$$U(\rho, z; \omega) = -\left(\frac{1}{2}(\omega\rho)^2 + \frac{\mu}{r}\right) \tag{17}$$

For a type-III equilibrium, where ρ and z are the free parameters,

$$|\mathbf{F}| = \sqrt[2]{\rho^2(\omega_0 - \omega_*)^2 + z^2\omega_*^4} \tag{18}$$

with the perturbation direction given by

$$\tan\alpha = \frac{\rho}{z}\left[1 - \left(\frac{\omega_0}{\omega_*}\right)^2\right] \tag{19}$$

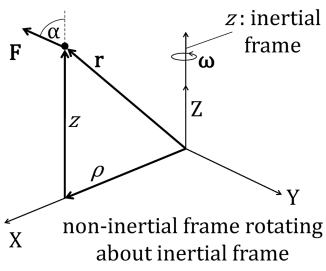

Fig. 2 Rotating polar coordinate system.

where $\omega_* = \sqrt[2]{(\mu/\rho^3)}$, $\omega_0 = \sqrt[2]{(\mu/r^3)}$, and r is the reference orbit radius against which the displaced orbit shall be synchronous.

To maintain a given repeat ground track, the vertical (or out-of-plane) displacement from the reference orbit is zero ($z = 0$) while the desired thrust is along the radial direction. Recall that the required thrust for a nonnatural sun-synchronous orbit is out of the orbit plane and hence decoupled from the thrust required for a displaced orbit. From Eq. (14) and Fig. 1 for an out-of-plane perturbation of a magnitude of 0.2 mm s^{-2} at $n = 14$ a sun-synchronous orbit can be achieved at an orbit altitude of 888 km and inclination of 98.2 or 99.8 deg, i.e., ± 0.79 deg, depending on the orientation of the low-thrust propulsion. Using Eq. (18) it is found that for a further orbit perturbation of a magnitude of 0.2 mm s^{-2}, in the radial direction, the orbit altitude can be varied by up to 64 m without altering the orbit period or ground track. Similarly, an altitude variation of 1 km can be achieved by a radial orbit perturbation of a magnitude of 3.1 mm s^{-2}. Clearly, large variations in the orbit altitude require prohibitively large acceleration magnitudes; however, small variations could be used for EO formation-flying applications, such as distributed synthetic aperture radar. Finally, it is noted that each of the above steps allows the spacecraft to move from simply occupying a length of space around the Earth (i.e., a standard orbit) 1) to an area of space defined as a segment of the surface of a sphere (i.e., variable inclination) and 2) to a volume of space defined as a segment of a thin-walled sphere (i.e., variable inclination and altitude), while always maintaining a constant ground track. Thus, the tracking of such an agile, unknown Earth observation (i.e., hostile military reconnaissance) spacecraft would be significantly more complex.

V. Numerical Simulation

The analytical analysis was examined within a numerical simulation for validity. The numerical simulation propagates the spacecraft position using an explicit variable-step-size Runge–Kutta [4,5] formula, the Dormand–Price pair (a single-step method) [9], to integrate the modified equinoctial equations of motion in Gauss form [10,11]. The spacecraft trajectory was propagated with consideration to lunar and solar gravity as point masses and the Earth's oblateness up to the 18th order (zonal and tesseral). No other perturbations are considered; however, the position of the sun was corrected for the eccentricity of Earth's orbit.

The ENVISAT spacecraft has a nominal ground-track repeat period of 35 days ($n = 14\frac{11}{35}$), giving a nominal altitude (assuming mean volumetric radius of Earth and a circular orbit) of 781 km and, for a natural sun-synchronous orbit, an inclination of 98.5 deg. From Eq. (14) and Fig. 1, if a continuous-low-thrust perturbation of a magnitude of 0.2 mm s^{-2} is considered, it is possible to fix the orbit

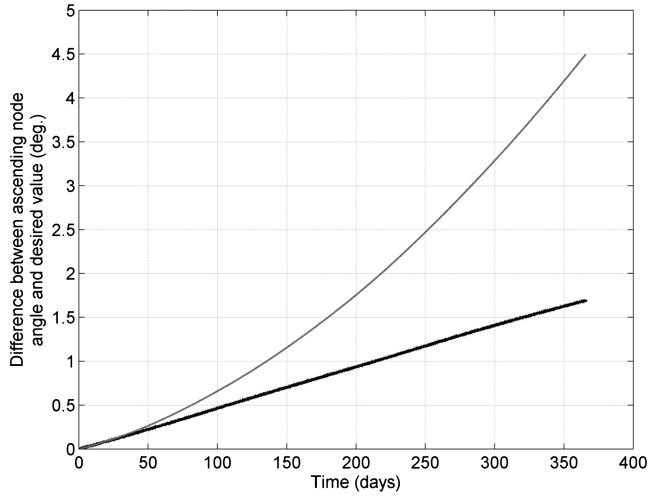

Fig. 3 Separation angle between ascending node and desired value; black line is a natural, uncontrolled, and sun-synchronous orbit, and gray line is nonnatural, uncontrolled, and sun-synchronous orbit.

inclination and vary the altitude by +190.2 to −165.9 km. However, such a variation would alter the repeat-ground-track period. Therefore, fixing the orbit altitude, the inclination can be varied by ±0.74 deg. Figure 3 shows the separation angle between the ascending node of a natural uncontrolled sun-synchronous orbit similar to that of ENVISAT and the desired value, along with the similar separation angle for an uncontrolled sun-synchronous orbit with the same repeat-ground-track period at an inclination of 97.8 deg, enabled by an acceleration magnitude of 0.2 mm s^{-2}. It is seen that both scenarios presented in Fig. 3 result in the ascending node angle rotating faster than desired. However, it is of note that the divergence of the nonnatural orbit from the desired state is nonlinear, as opposed to the natural orbit. It is of further note that the inclination, not shown, exhibits a long-period oscillation in the natural sun-synchronous orbit, due to third-body gravity effects. However, in the forced scenario, while the inclination maintains a long-period oscillation, the trend is a near-linear incremental drift of just over +0.1 deg in the year.

An orbit displaced +50 m in the radial direction from the above nonnatural sun-synchronous orbit but with the same orbit period is now considered: i.e., a type-III displaced orbit. The initial conditions of such a numerical simulation must be carefully considered, as the orbital velocity must be set to conserve the angular velocity of the reference orbit. From Eq. (18), an orbit perturbation of a magnitude of 0.16 mm s^{-2} is required in the negative radial direction. In addition, an orbit perturbation of a magnitude of $(0.2 + 5.101e - 5)$ mm s^{-2} out of the orbit plane is required to enable the sun-synchronous rotation; the additional term in the out-of-plane perturbations accounts for the additional altitude of the displaced spacecraft. Figure 4 shows the uncontrolled separation distance between a spacecraft on the displaced orbit and a reference spacecraft on the nonnatural sun-synchronous orbit over a 12 h period. Figure 4 shows that the interspacecraft distance drops below 45 m on the first orbit, with the interspacecraft distance oscillation magnitude increasing over subsequent orbits. The ascending node angle of the displaced spacecraft after 60 days was found to have drifted less than one arcminute behind the nonnatural sun-synchronous orbit. It is of note that if the orbit perturbations are removed and only the above radial perturbation applied to the displaced spacecraft the interspacecraft distance varies within the bounds of the numerical calculation error, therefore clearly suggesting that a simple control system should be able to maintain the nominal interspacecraft distance through the use of further low thrust. Finally, the scenario presented in Fig. 4 was repeated for a spacecraft displaced from the ENVISAT orbit, requiring only the radial thrust component to maintain the orbit displacement, and found to replicate Fig. 4 to a very high level of precision.

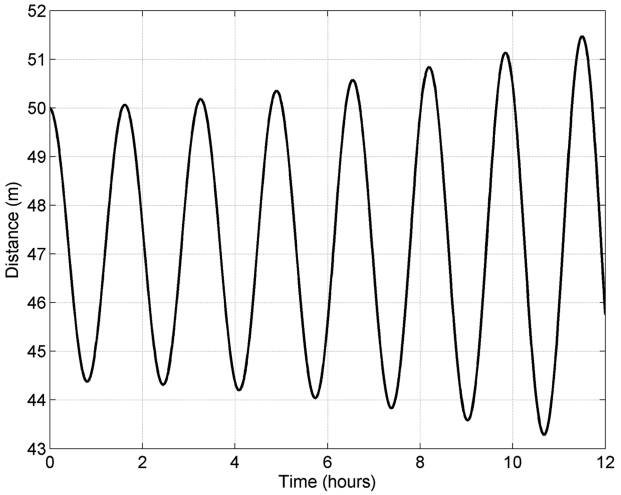

Fig. 4 Interspacecraft distance between an ENVISAT-like nonnatural sun-synchronous orbit and a second spacecraft on a type-III, 50 m displaced orbit.

The transfer to the displaced orbit has been split into two maneuvers: an asynchronous transfer from an inclination of 98.5 deg to an inclination of 97.8 deg and a synchronous transfer from the orbit at 97.8 deg of inclination to an orbit with equal inclination but an altitude increased of 50 m. The low-thrust transfer was performed with a direct transcription method based on finite elements in time generated on spectral basis [12,13]. The equinoctial equations of motion in Gauss form were used to describe the spacecraft motion [10,11]. The specific impulse of the engine was set to 3000 s, and the maximum thrust level was set to 0.258 N on an initially 1000 kg spacecraft.

The asynchronous inclination change means that the spacecraft reaches the new inclination with a small phase difference with respect to the departure orbit. The inclination change takes 257 h and requires 3.8 kg of propellant. The altitude change is synchronous and is performed over one full revolution, about 1.67 h, and requires 53 g of propellant.

VI. Discussion

Recently, the Committee on Earth Observation Satellites and the Global Climate Observing System identified 21 fundamentally important essential climate variables that are largely dependent on space-based EO [14]. Essential climate variables are required for the validation of, and assimilation into, Earth system models to predict future climate change, and thus the scarce resource of preferred sun-synchronous orbits will become increasingly sought after for future EO missions. The use of low-thrust propulsion considered herein enables enhanced EO mission opportunities with currently available, or near-term, technology such as the QinetiQ T6 thruster, which will provide a thrust up to 230 mN at a specific impulse above 4500 s for the BepiColombo mission [15].

Considering the application of extending the sun-synchronous orbit, it is noted that the ENVISAT orbit was selected for a variety of reasons, including instrument swath width for rapid global coverage and spacecraft operations. Among the reasons for the ENVISAT orbit, however, is the desire to maintain continuous data collection from the profiling instruments, the Microwave Radiometer, and the radar altimeter 2, which do not provide real global coverage but span a tight grid of measurements over the globe, first established by European Remote Sensing satellites 1 and 2 (ERS-1 and ERS-2). Such long-term continuous data collection is critical for validation and assimilation into Earth system models to predict future climate change and, as such, a change of orbit degrades the data set. However, positioning a second spacecraft beside the nominal orbit, as demonstrated above, enhances the data set by enabling the tight grid of measurements to be expanded. The application of the extended sun-synchronous orbit is thus twofold, enabling sun-synchronous orbits at new orbit inclinations and enabling sun-synchronous orbits on a given repeat ground track at new orbit altitudes or inclinations to enhance the data set collection of existing EO missions.

From Eq. (5) it is seen that the rate of change of the ascending node angle varies as the sinusoidal function of the argument of latitude. Therefore, assuming a circular orbit, the rate of change of the ascending node angle is zero at equatorial crossings, regardless of the out-of-plane force applied. As such, any thrusting by the spacecraft within this region would be highly inefficient, and spacecraft thrusting should be focused about the polar regions of the orbit. Note that such coast arcs require the thrust magnitude to be increased such that the total delivered force about the orbit remains constant; however, it can be shown that a coast arc of 25 deg on either side of the equator requires the force magnitude to be increased by less than 5%. Furthermore, the thrust direction switching law described and used above could be replaced by a unidirectional thrust, for example, an attitude fixed solar sail, using an eccentric orbit with pericenter located over a planetary pole. On such an orbit, the rate of change of the ascending node would be unbalanced about the semilatus rectum/equatorial crossing, giving a secular variation in ascending node angle. Such a scenario is analogous to the Mercury sun-synchronous concept, in which a solar sail provides the required orbit perturbations

for a sun-synchronous orbit at Mercury, which is otherwise not possible due to Mercury's high reciprocal of flattening [16].

VII. Conclusions

It has been shown that the analytical derivation of the sun-synchronous orbit can be extended to allow free selection of the orbit inclination and semimajor axis for a given repeat ground track. The analytical derivation was considered using a numerical simulation, which showed that the extended and displaced sun-synchronous orbit was valid. It was also shown that the required propellant to inject a spacecraft into such orbits was easily tolerable. The level of thrust required to maintain either an extended sun-synchronous orbit or a displaced sun-synchronous orbit was shown to be consistent with near-term technology under development for future planned missions, including the BepiColombo mission.

Acknowledgment

This work was partly funded by ESA contract number 22349/09/F/MOS (Study on Gravity Gradient Compensation Using Low-Thrust High-I_{sp} Motors).

References

[1] Roy, A. E., *Orbital Motion*, 4th ed., Taylor & Francis, London, 2005, Chaps. 7, 11.

[2] Vallado, D. A., *Fundamentals of Astrodynamics and Applications*, 3rd ed., Springer, New York, 2007, Chap. 11.

[3] Duesmann, B., and Barat, I., "ERS-2 and ENVISAT Orbit Control: Current and Future Strategy—The Impact on the Interferometric Baselines," *FRINGE 2007 Workshop*, ESA, Nov. 2007.

[4] Frerick, J., Duesmann, B., and Canela, M., "2010 and Beyond—The ENVISAT Mission Extension," *ENVISAT Symposium 2007*, SP-636, ESA, 23–27 April 2007, July 2007.

[5] McInnes, C. R., *Solar Sailing: Technology, Dynamics and Mission Applications*, Springer-Praxis, Chichester, England, U.K., 1999, p 120.

[6] Macdonald, M., and McInnes, C. R., "Analytical Control Laws for Planet-Centred Solar Sailing," *Journal of Guidance, Control, and Dynamics*, Vol. 28, No. 5, 2005, pp. 1038–1048. doi:10.2514/1.11400

[7] McInnes, C. R., "Dynamics, Stability and Control of Displaced Non-Keplerian Orbits," *Journal of Guidance, Control, and Dynamics*, Vol. 21, No. 5, 1998, pp. 799–805. doi:10.2514/2.4309

[8] McKay, R., Macdonald, M., Bosquillon de Fresheville, F., Vasile, M., McInnes, C., and Biggs, J., "Non-Keplerian Orbits Using Low-thrust, High I_{sp} Propulsion Systems," 60th International Astronautical Congress, IAC Paper 09.C1.2.8, Daejeon, ROK, Oct. 2009.

[9] Dormand, J. R., and Price, P. J., "A Family of Embedded Runge–Kutta Formulae," *Journal of Computational and Applied Mathematics*, Vol. 6, 1980, pp. 19–26. doi:10.1016/0771-050X(80)90013-3

[10] Walker, M. J. H., Ireland, B., and Owens, J., "A Set of Modified Equinoctial Elements," *Celestial Mechanics*, Vol. 36, 1985, pp. 409–419. doi:10.1007/BF01227493

[11] Betts, J. T., "Optimal Interplanetary Orbit Transfers by Direct Transcription," *Journal of the Astronautical Sciences*, Vol. 42, No. 3, July–Sept. 1994, pp. 247–268.

[12] Vasile, M., and Bernelli-Zazzera, F., "Targeting a Heliocentric Orbit Combining Low-Thrust Propulsion and Gravity Assist Manoeuvres," *Operations Research in Space and Air, Applied Optimization*, Vol. 79, Kluwer Academic, Norwell, MA, 2003.

[13] Vasile, M., and Bernelli-Zazzera, F., "Optimizing Low-Thrust and Gravity Assist Manoeuvres to Design Interplanetary Trajectories," *Journal of the Astronautical Sciences*, Vol. 51, No. 1, Jan.–March 2003, pp. 13–35.

[14] "Global Monitoring of Essential Climate Variables," ESA Earth Observation Programme Board, Rept. PB-EO(2009)32, Feb. 2009.

[15] Wallace, N., "Testing of the QinetiQ T6 Thruster in Support of the ESA BepiColombo Mercury Mission, *Proceedings of the 4th International Spacecraft Propulsion Conference* [CD-ROM], edited by A. Wilson, SP-555, ESA, 2–9 June, 2004; also http://articles.adsabs.harvard.edu/full/2004ESASP.555E..70W [retrieved 24 Aug. 2009].

[16] Leipold, M. E., and Wagner, O., "Mercury Sun-Synchronous Polar Orbits Using Solar Sail Propulsion," *Journal of Guidance, Control, and Dynamics*, Vol. 19, No. 6, 1996, pp. 1337–1341. doi:10.2514/3.21791